Ab initio and density functional study of barrier heights of methyl group torsion and hyperconjugation in 1,2,3,5-tetramethylnaphthalene

R. Meenakshi [a*] T.Umadevi [b] A. Josephine Prabha [c] P,Thandeswari [a]

[a] *PG Department of Physics,Cauvery College For Women,Tiruchirappalli – 620 018, India*
[b]*Department of Physics, Government Arts College for Women, Pudukkottai, India*
[c] *Department of Physics,Bishop Heber College,Trichy- India*

Corresponding author. R.Meenakshi,. *E-mail address:*lr.santhameena@gmail.com

Abstract

Toxic, mutagenic and carcinogenic effects among **tetramethylnaphthalene** (TMN) may differ considerably and for that reason it is important to identify all changes in their structures. We have reported the results of ab initio and DFT calculations of equilibrium molecular geometry, vibrational spectrum and assignments in the ground electronic state of 1,2,3,5-tetramethylnapthalene(1,2,3,4-TMN). The structural parameters of 1,2,3,5-tetramethylnapthalene are analyzed and compared with those of the naphthalene molecule. The rotational barriers heights of 1,2,3,5-tetramethylnapthalene are determined. For comparison, the barrier heights of 1-methylnapthalene(1-MN) and 2-methylnapthalene (2-MN) are calculated using the same methods and they are in good agreement with the experimental values. In the HOMO and LUMO of 1,2,3,5-tetramethylnapthalene ,a type of orbital interaction named π^*-σ^* hyperconjugation discovered earlier by Nakai and Kawamura [1], is also observed. The variations of the rotational barriers in the S0 state of 1,2,3,5-tetramethylnapthalene are shown to be directly connected with the stability of HOMO and the orbital's stability is determined by π^*-σ^* hyperconjugation. The present study will aid to the identify the intermolecular interactions of 1,2,3.4-TMN with other biomolecules and molecules in the environment in general.

1 Introduction

Naphthalene derivatives have many applications in industrial processes. They are important intermediates for pharmaceutical, construction, agricultural, rubber, and textile chemicals. On the other hand, alkylated naphthalene derivatives are widespread environmental pollutants. Tetramethylnapthalenes and Trimethylnaphthalenes as well as other alkylated naphthalenes such as

methyl- and dimethylnaphthalenes are components of diesel fuel and residues of oil product refining. Various TMNs are among alkylated naphthalenes which are main volatile PAHs of bitumen emissions. The results of Lindberg et al. [1] suggest that fumes from asphalt mixed with recycled additives contain direct-acting genotoxic components. It is widely recognized that methylation can induce, enhance, reduce or abolish the toxic, carcinogenic, or mutagenic properties of PAHs. Methyl substitution in PAHs can alter their carcinogenic activity depending on the number of substituents and on the position of substitution [2]. Small changes in structure can have a large effect on carcinogenic activity. It is essential therefore to investigate changes of structural and electronic properties of PAHs that methyl substituents cause. Although TMNs as well as other alkylated naphthalenes are widespread environmental pollutants among PAHs, the information on TMNs is sparse. The IR spectra of four trimethylnaphthalenes (1,3,5-, 1,3,8-, 1,4,5-, and 1,6,7-TMN) were reported by Mosby [3]. The IR spectra of 13 trimethylnaphthalene isomers were reported by Meyer and Duswalt [4] but complete vibrational assignments have not been made.

A semiempirical study and experimental results of electronic excitation energies of some TMN isomers were reported [5]. Wasserman et al., [6] optimized at the B3LYP/6-311+G* level the geometries of two isomers (1,4,5-TMN and 1,2,4-TMN). Taking into account the small number of reported papers on trimethylnaphthalenes, in this work, the first theoretical report on geometry, vibrational frequencies, IR intensities, Raman activities, and barrier heights to internal rotation of methyl groups in the ground electronic state (S0) of the 1,2,3,5-tetramethylnathalene (1,2,3,5-TMN). Internal rotation in molecules may have a significant effect on the non-covalent interactions and each of the three methyl groups in a TMN can have a different effect. The π*-σ* hyperconjugation (HC), discovered by Nakai and Kawai appears between an unoccupied benzene π* orbital and an unoccupied σ* orbital of the C-H bond in the methyl group [7–9]. The model was successfully applied to explain the stability of the highest occupied molecular orbital (HOMO) and the lowest unoccupied molecular orbital (LUMO) of substituted toluenes and methylnaphthalenes. Here, the π*– σ* hyperconjugation effects in 1,2,3,5-tetramethylnaphthalene (1,2,3,5-TMN) and their influence on the torsional barriers in the ground electronic state have been investigated.

2. Computational details

The geometry optimization of 1,2,3,5-TMN in the ground electronic state and its rotamers is carried out using ab initio Hartree– Fock (HF) and DFT calculations. The geometries were fully optimized by the B3LYP (Becke3–Lee–Yang–Parr) method [10,11] with a correlation-consistent polarized valence triple-zeta basis set, cc-pVTZ [12]. The optimized structural parameters are used for the vibrational frequency calculation. The frequency calculations were carried out at the same level as the geometry optimization using analytic evaluation of the second derivatives of energy

with respect to the nuclear displacements. The frequency B3LYP calculation of the equilibrium geometry of 1,2,3,5-TMN isomer showed no imaginary values, implying that the structure is minimum on the potential energy surface. Four transition states (TSs) structures of four rotamers (see Figure 1) are characterized by one imaginary frequency which is 80i for all rotamers .

The assignment of vibrational modes was carried out on the basis of normal modes as displacements in redundant internal coordinates and through the GAUSS VIEW visualization program. The investigated molecule is a tetra rotor case. The Hartree–Fock (HF) method is employed for the calculations of methyl group torsional barriers.

3. Results and discussion

3.1. Optimized parameters of 1,2,3,5-TMN isomer and Theoretical vibrational assignments

The fully optimized molecular geometries of the 1,4,6-TMN isomer and transition state structures of rotamers obtained at the B3LYP/ cc-pVTZ level, along with the labeling of atoms are displayed in Figure 1. The selected optimized geometrical parameters of the investigated isomer obtained at the B3LYP/ cc-pVTZ level, its rotamers and comparison with the corresponding values of the naphthalene molecule calculated at the same level of theory are given in Table 1. The structural changes that one methyl substituent introduces into the naphthalene ring are not confined to the methylated ring [13].

The major structural change is found for the bond length between C10 and the carbon atom bound to the methyl group in position C4. The computed bond length C4-C10 is 0.0023Å larger than the corresponding bond length (1.416 Å) in the naphthalene molecule fully optimized at the same level of theory. The similar effect on the C-C bond length of the ring system is found for another methyl group in position C1: the C1-C9 bond length is 0.021Å larger than the corresponding C-C bond length in the naphthalene molecule. The most remarkable changes of the bond angles from those in the naphthalene molecule can be noticed for the angles C8-C9-C1 and C4-C10-C5. The C4-C10-C5 bond angle of 1,2,3,5-TMN is smaller (121.9569˚), than the corresponding angle in naphthalene, 122.33˚. On the other hand, compared to the C8-C9-C1 bond angle in the naphthalene molecule (122.33˚), the corresponding angle in the 1,2,3,5-TMN is 122.0608˚. The geometries of the ground state of 1,2,3,5-TMN and TS structures of the corresponding rotamers are reasonably close to each other. The theoretical IR and Raman spectra are shown in Figs 2 and 3, respectively. The corresponding detailed vibrational assignments are shown in Table 2.

3.2. Internal rotation of the methyl groups in 1,2,3,5-TMN, 1,4,6-TMN ,1-MN and 2-MN

The 1,2,3,5-TMN is a four-rotor molecule regarding the internal rotational motion of the methyl groups. The torsional barrier heights in the ground electronic state of 1,2,3,5-TMN for four

rotamers are calculated as the difference between the energy of the minimum of the equilibrium structure and the energy of the TS structure of the corresponding rotamers (Table 3). The table also includes the barriers heights of 1,4,6-TMN, 1-MN and 2-MN calculated as the energy difference between the minimum and TS structure which are taken from the work of B.D. Ostoji´ et al., [14] for comparative study. The experimental values are also presented in the Table 3. The results of the calculations have shown that both minimum energy structure and transition energy structures of rotamers 1, 2, 3 and 4 of 1,2,3,5-TMN have the methyl group oriented so that two C-H bonds are approximately staggered with respect to the plane of naphthalene rings while the third C-H bond is approximately eclipsed. The minimum energy structure of 1,2,3,5-TMN is the conformation in which two hydrogen atoms on the left-hand side (counterclockwise) of the methyl groups attached to the first and the second positions are staggered while one hydrogen atom on the right-hand side (clockwise) of the corresponding methyl groups is eclipsed with respect to the ring plane (Figure 1). The conformations characterized by two hydrogen atoms on the right-hand side of the methyl group staggered and one hydrogen on the left-hand side eclipsed are the transition state structures of the rotamers (Figure 1).

The calculated barrier heights of 1-MN and 2-MN are 667 and 207 cm^{-1}, respectively, and they are in reasonable agreement with the measured value obtained from rotationally resolved fluorescence excitation spectra of 1-MN and 2-MN, 809 and 234 cm^{-1}, respectively [15].

As expected, in this two-ring system characterized by the asymmetry about the rotor axes, each barrier height is different. The rotamer 1 has higher value of the barrier height, 809 cm^{-1}, than the other rotamers, 194 cm^{-1}, in correlation with higher values of the barrier heights of 1-MN compared to the barrier height of 2-MN [5]. The barrier height of the rotamer 2 is higher than other rotamer. The rotamer 4 possesses lower barrier height, 567 cm^{-1}, compared to the barrier height of 1-MN, 667 cm^{-1}.

3.3. Hyperconjugation (HC) effects in 1,2,3,5-TMN

Similar to the hyperconjugation effects in 1-MN and 2-MN [16] where π^*-σ^* HC appears in HOMOs and LUMOs, we examined the π^*-σ^* hyperconjugation effects in 1,2,3,5-TMN. The electron density plots of HOMO and LUMO in 1,2,3,5-TMN and in the corresponding transition state structures of the rotamers are shown in Figure 3.The stability of HOMO and LUMO for rotamers 1 and 3, consistent with the great π^*-σ^* HC interaction comparatively than other rotamers due to the shortest average distance between methyl group hydrogen and the corresponding nearest ring hydrogen of rotamers 1 and 3.

4 Conclusion

Toxic, mutagenic and carcinogenic effects among TMNs may differ considerably and for that reason it is important to identify all changes in their structures. We have reported the results of ab initio and DFT calculations of equilibrium molecular geometry, vibrational spectrum and assignments in the ground electronic state of 1,2,3,5-tetramethylnapthalene. The structural parameters of 1,2,3,5-tetramethylnapthalene are analyzed and compared with those of the naphthalene molecule. The calculated frequencies are in good agreement with the available experimental data. Different techniques have been used to determine the rotational barriers heights of 1,2,3,5-tetramethylnapthalene. For comparison, the barrier heights of 1-MN and 2-MN are calculated using the same methods and they are in good agreement with the experimental values. In the HOMO and LUMO of 1,2,3,5-tetramethylnapthalene a type of orbital interaction named π^*-σ^* hyperconjugation discovered earlier by Nakai and Kawamura [8], is also observed. The variations of the rotational barriers in the S0 state of 1,2,3,5-tetramethylnapthalene are shown to be directly connected with the stability of HOMO and the orbitals stability is determined by π^*-σ^* hyperconjugation. The present study will help in the identification of the intermolecular interactions of this molecule with other biomolecules and molecules in the environment in general.

References

[1] H.K. Lindberg et al., Mutat. Res. 653 (2008) 82.

[2] D.W. Jones, R.S. Matthews, in: G. Ellis, G.B. West (Eds.), Progress in Medicinal Chemistry, North-Holland, Amsterdam, 1974, p. 159.

[3] W.L. Mosby, J. Am. Chem. Soc. 74 (1952) 2564.

[4] T.J. Mayer, J.M. Duswalt, J. Chem. Eng. Data 18 (1973) 337.

[5] N. Mora-Diez, R.J. Boyd, G.L. Heard, J. Phys. Chem. A 104   (2000)1020.

[6] H.H. Wasserman, K.B. Wiberg, D.L. Larsen, J. Parr, J. Org. Chem. 670 (2005) 105.

[7] H. Nakai, M. Kawai, Chem. Phys. Lett. 307 (1999) 272.

[8] H. Nakai, Y. Kawamura, Chem. Phys. Lett. 318 (2000) 298.

[9] H. Nakai, M. Kawai, J. Chem. Phys. 113 (6) (2000) 2168.

[10] C. Lee, W. Yang, R.G. Parr, Phys. Rev. B 37 (1988) 785.

[11] A.D. Becke, J. Chem. Phys. 98 (1993) 5648.

[12] T.H. Dunning Jr., J. Chem. Phys. 90 (1989) 1007.

[13] P. George, C.W. Bock, J.J. Stezowski, T. Hildenbrand, J.P. Glusker, J.Phys.Chem.92 (1988) 5656.

[14] Bojana D. Ostojic´, Dragana S. Đord-evic´, dx.doi.org/10.1016/j.cplett.2012.03.078

[15] X.-Q. Tan, W.A. Majewski, D.F. Plusquellic, D.W. Pratt, J.Chem. Phys. 94 (1991) 7721.

[16] D.N. Sathyanarayana, Vibrational Spectroscopy – Theory and Applications, New Age
      International Publishers, New Delhi, (2004).

IJSER

Table 1

Optimized parameters of 1,2,3,5-tetramethylnapthalene by B3LYP method using cc-pVTZ basis set

Atoms	Bond length (Å)		Atoms	Bond angles(°)		Atoms	Dihedral angles (°)
	1,2,3,5-TMN	NPH [a]		1,2,3,5-TMN	NPH		
C1-C2	1.3938	1.3702	C2-C1-C9	120.4998	120.87	C9-C1-C2-C3	0.0047
C1-C9	1.437	1.4160	C2-C1-C15	121.1668	-	C9-C1-C2-C19	-179.9971
C1-C15	1.5162	-	C9-C1-C15	118.3333	-	C15-C1-C2-C3	180.001
C2-C3	1.4353	1.4116	C1-C2-C3	119.7849	120.30	C15-C1-C2-C19	-0.0008
C2-C19	1.5194	-	C1-C2-C19	120.6056	-	C2-C1-C9-C8	179.9956
C3-C4	1.38	1.3702	C3-C2-C19	119.6095	-	C2-C1-C9-C10	-0.0028
C3-C23	1.5151	-	C2-C3-C4	119.6327	120.30	C15-C1-C9-C8	-0.0008
C4-C10	1.4183	1.4160	C2-C3-C23	121.4225	-	C15-C1-C9-C10	-179.9992
C4-H12	1.0811	-	C4-C3-C23	118.9448	-	C2-C1-C15-H16	0.0141
C5-C6	1.3822	1.3702	C3-C4-C10	122.465	120.87	C2-C1-C15-H17	120.3939
C5-C10	1.4365	1.4160	C3-C4-H12	118.5134	-	C2-C1-C15-H18	-120.3649
C5-C27	1.5122	-	C10-C4-H12	119.0216	-	C9-C1-C15-H16	180.0105
C6-C7	1.4135	1.3702	C6-C5-C10	119.0351	120.87	C9-C1-C15-H17	-59.6097
C6-H13	1.0829	-	C6-C5-C27	120.1918	-	C9-C1-C15-H18	59.6315
C7-C8	1.3765	1.3702	C10-C5-C27	120.7731	-	C1-C2-C3-C4	-0.0032

C7-H14	1.0824	-	C5-C6-C7	121.3079	120.30	C1-C2-C3-C23	179.996
C8-C9	1.4253	1.4160	C5-C6-H13	119.3993	-	C19-C2-C3-C4	-180.0014
C8-H11	1.0798	-	C7-C6-H13	119.2928	-	C19-C2-C3-C23	-0.0023
C9-C10	1.434	1.4283	C6-C7-C8	120.4565	120.30	C1-C2-C19-H20	-59.9756
C15-H16	1.0856	-	C6-C7-H14	119.4705	-	C1-C2-C19-H21	59.9137
C15-H17	1.0935	-	H8-H7-H14	120.073	-	C1-C2-C19-H22	179.9697
C15-H18	1.0935	-	C7-C8-C9	120.8359	-	C3-C2-C19-H20	120.0226
C19-H20	1.0929	-	C7-C8-H11	119.3769	-	C3-C2-C19-H21	-120.0881
C19-H21	1.0929	-	C9-C8-H11	119.7873	-	C3-C2-C19-H22	-0.0321
C19-H22	1.0861	-	C1-C9-C8	122.0608	120.33	C2-C3-C4-C10	-0.0003
C23-H24	1.0932	-	C1-C9-C10	119.527	118.83	C2-C3-C4-H12	-180.0005
C23-H25	1.0932	-	C8-C9-C10	118.4122	118.83	C23-C3-C4-C10	-179.9995
C23-H26	1.0899	-	C4-C10-C5	121.9569	122.33	C23-C3-C4-H12	0.0004
C27-H28	1.0935	-	C4-C10-C9	118.0906	118.83	C2-C3-C23-H24	-60.2582
C27-H29	1.0935	-	C5-C10-C9	119.9525	118.83	C2-C3-C23-H25	60.2731
C27-H30	1.0899	-	C1-C15-H16	112.3749	-	C2-C3-C23-H26	-179.9929
			C1-C15-H17	111.3128	-	C4-C3-C23-H24	119.741
			C1-C15-H18	111.3127	-	C4-C3-C23-H25	-119.7278
			H16-C15-H17	107.2964	-	C4-C3-C23-H26	0.0063
			H16-C15-H18	107.2959	-	C3-C4-C10-C5	-179.9979
			H17-C15-H18	106.969	-	C3-C4-C10-C9	0.0022
			C2-C19-H20	111.668	-	H12-C4-C10-C5	0.0022

			C2-C19-H21	111.6692	-	H12-C4-C10-C9	-179.9977
			C2-C19-H22	111.9474	-	C10-C5-C6-C7	-0.0016
			H20-C19-H21	107.1006	-	C10-C5-C6-H13	179.9993
			H20-C19-H22	107.0799	-	C27-C5-C6-C7	179.9962
			H21-C19-H22	107.0803	-	C27-C5-C6-H13	-0.0029
			C3-C23-H24	112.0973	-	C6-C5-C10-C4	180.0009
			C3-C23-H25	112.0974	-	C6-C5-C10-C9	0.0008
			C3-C23-H26	110.3875	-	C27-C5-C10-C4	0.0032
			H24-C23-H25	107.1339	-	C27-C5-C10-C9	-179.9969
			H24-C23-H26	107.4405	-	C6-C5-C27-H28	119.9407
			H28-C27-H30	107.6161	-	C5-C6-C7-C8	0.0005
			H29-C27-H30	107.6159	-	C5-C6-C7-H14	-179.9989

[a] Ref [37]

Table 2

Assignments of calculated frequencies of 1,2,3,5-tetramethylnapthalene by B3LYP method using cc-pVTZ basis set.

S.No	Frequency (cm^{-1})	IR Intensity	Raman Activity	Assignments with % of TED
1	3203	27.3842	146.5358	CH$_3$ips(98)
2	3181	18.3833	71.5134	CH$_3$ips(97)
3	3176	37.9895	190.6071	CH$_3$ips(99)
4	3157	14.1855	81.8771	CH$_3$ips(97)
5	3140	17.6918	58.1091	CH$_3$ss(98)
6	3134	32.5445	66.3998	CH$_3$ss(98)
7	3095	24.5969	74.8169	CH$_3$ss(99)
8	3094	26.3569	61.5090	CH$_3$ss(98)
9	3061	11.3832	61.1939	CH$_3$ops(97)
10	3058	34.5178	117.8619	CH$_3$ops(98)
11	3056	54.6541	8.6508	CH$_3$ops(98)
12	3057	0.4458	156.5739	CH$_3$ops(97)
13	3016	34.5178	117.8619	vCH(95)
14	3013	54.6541	8.6508	vCH(96)
15	3009	0.4458	156.5739	vCH(97)
16	3007	35.5919	151.0784	vCH(95)
17	1658	1.1053	6.1134	vC=C(83)
18	1641	15.9787	15.9757	vC=C(86)
19	1614	0.6882	74.8593	vC=C(84)
20	1560	0.1389	2.4096	vC=C(83)
21	1553	14.7230	6.5619	vC=C(84)
22	1548	12.5424	8.7592	vC-C(83)
23	1542	6.4038	37.9658	vC-C(86)
24	1540	1.1708	22.8240	vC-C(89)
25	1534	17.1998	2.1965	vC-C(84)
26	1530	8.0489	21.4552	vC-C(85)
27	1525	25.1070	22.6459	vC-C(83)
28	1511	1.7090	4.2430	vC-C(82), vC-C (16)
29	1491	9.1852	4.2416	vC-C(80), bCH(16)
30	1470	2.7866	2.7071	vC-C(87), bCH(16)
31	1457	4.2175	71.0523	vC-C(79),vC-C(21)
32	1455	6.6923	19.8861	CH$_3$ipb(98)

33	1451	9.7085	41.0392	$CH_3ipb(98)$
34	1448	6.0091	22.6748	$CH_3ipb(98)$
35	1418	7.0316	41.4381	$CH_3ipb(98)$
36	1398	1.5437	207.8035	$CH_3sb(97)$
37	1357	1.0785	1.2121	$CH_3sb(97)$
38	1309	0.4785	0.4011	$CH_3sb(97)$
39	1275	0.4774	1.7539	$CH_3sb(97)$
40	1260	5.5732	2.7947	$CH_3opb(98)$
41	1220	1.1647	3.4411	$CH_3opb(98)$
42	1215	2.0750	8.7954	$CH_3opb(98)$
43	1133	0.2459	1.8991	$CH_3opb(98)$
44	1106	7.5637	4.2045	$bCH(79)$, $R_1symd(17)$
45	1098	0.6935	0.3235	$bCH(61)$, $\upsilon C\text{-}C(23)$
46	1095	10.4249	7.4691	$bCH(57)$,$R_1asymd(22)$
47	1092	1.8331	0.1139	$bCH(59)$, $R_2symd(22)$
48	1088	1.4153	0.5799	$R_1asymd(71)$,$bCH(19)$
49	1062	3.3068	0.9244	$R_2asymd(71)$,$bNH(14)$
50	1049	3.8601	1.9657	$R_1symd(71)$,$R_2symd(22)$
51	1043	2.0632	8.6709	$R_2symd(71)$,$R_1symdd1(22)$
52	1004	0.4593	0.9579	$R_1trigd(76)$,$R_2symd(11)$
53	993	3.0338	3.0794	$R_2trigd(77)$,$R_2symd(11)$
54	927	0.8008	0.5891	$CH_3ipr(78)$
55	920	0.0331	5.4814	$CH_3ipr(88)$
56	906	16.3584	0.3928	$CH_3ipr(77)$
57	880	0.7572	4.1785	$CH_3ipr(78)$
58	817	30.5193	0.5294	$bCC(67)$, $tRasymd(20)$
59	790	1.6729	0.3148	$bCC(62)$,$bCH(19)$
60	769	17.5295	1.2001	$bCC(69)$, $bCH(22)$
61	693	1.2657	9.3131	$bCC(66)$, $bCH(24)$
62	691	0.5756	0.0923	$CH_3opr(79)$
63	593	0.7593	0.0566	$CH_3opr(75)$
64	591	0.2525	2.0679	$CH_3opr(76)$
65	566	0.8773	22.8702	$CH_3opr(74)$
66	550	3.7658	2.0549	$\delta CH(65)$, $\delta CC(20)$
67	549	0.0442	0.3151	$\delta CH(64)$, $tRasymd(21)$
68	504	0.6625	4.1045	$\delta CH(64)$,$\delta CC(16)$
69	468	1.7662	6.2237	$\delta CH(69)$, $\delta CC(22)$

70	441	0.4998	10.7329	tR$_1$trigd(51), tR$_3$asymd(15)
71	388	0.0925	0.2457	tR$_2$trigd(54),tR$_2$asymd(17)
72	359	0.7209	5.9810	tR$_1$symd(53),
73	337	0.6021	3.1315	tR$_2$symd(53),δCH(12)
74	331	0.0354	0.2135	tR$_1$asymd(55),δCH(12)
75	313	3.9808	0.3894	tR$_2$asymd(57),δCH(13)
76	232	0.5824	0.3203	δCC(64), tRasymd(18)
77	229	0.0138	1.0698	δCC(63), tRasymd(20)
78	215	0.1215	3.8565	δCC(62),δCH(19)
79	185	1.0237	0.0456	δCC(65), δCH(22)
80	163	1.2414	0.8706	tCH$_3$(56)
81	144	1.3204	0.6571	tCH$_3$(54)
82	118	1.9410	0.2293	tCH$_3$(55)
83	80	0.0809	0.3800	tCH$_3$(57)
84	70	0.0044	0.6118	Butterfly(64)

Abbreviations : υ - stretching; b - bending; symd - symmetric deformation; t – torsion

asymd - asymmetric deformation; trigd-trigonal deformation; δ-out of plane bending.

Table 3

Calculated and experimental internal rotation barrier heights (in cm^{-1}) of 1,2,3,5-tetramethylnapthalene(1,2,3,5-TMN),1-methylnapthalene(1-MN), and 2- methylnaphthalene(2-MN) using the B3LYP/cc-pVTZ optimized geometries.

Method	1,2,3,5- tetramethylnapthalene				1-MN	2-MN
	Rotamer1	Rotamer2	Rotamer3	Rotamer4		
B3LYP/cc-Pvtz	809	956	878	567	667[a]	207 [a]
Exp.[b]	-	-	-	-	809 [b]	234 [b]

[a] Ref [37]

[b] Ref. [38], rotationally resolved fluorescence excitation spectra.
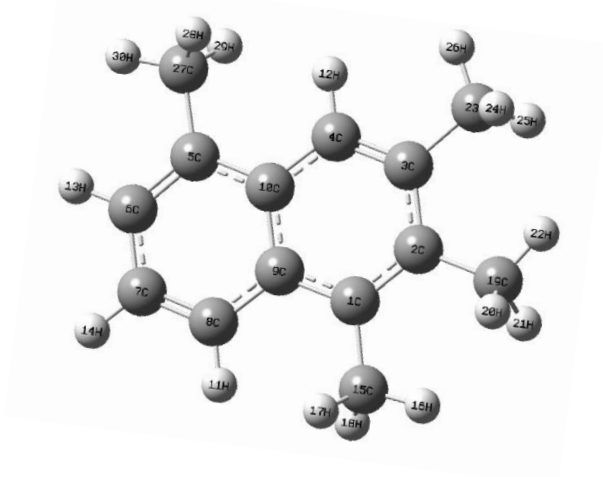
(a) Optimized structure of 1,2,3,5-tetramethylnapthalene
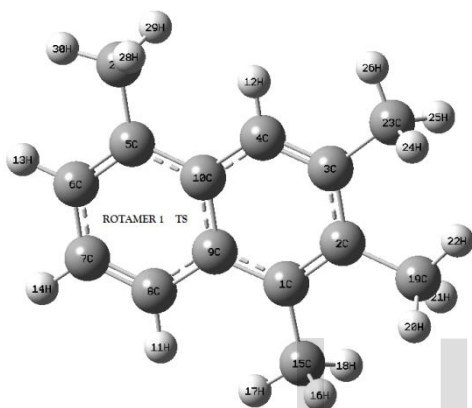
(b)Transition structure of Rotamer 1
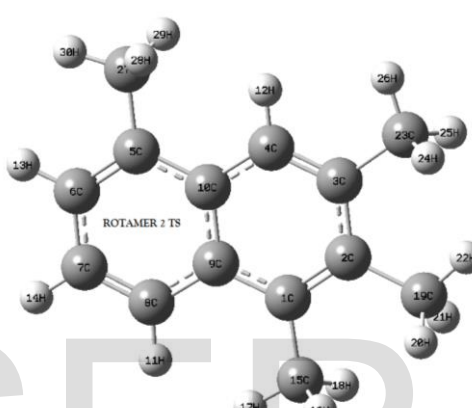
(c) Transition structure of Rotamer 2
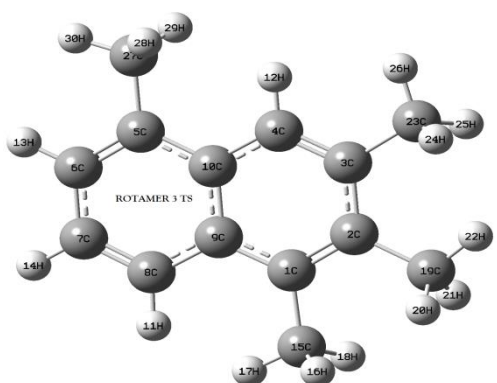
(d) Transition structure of Rotamer 3
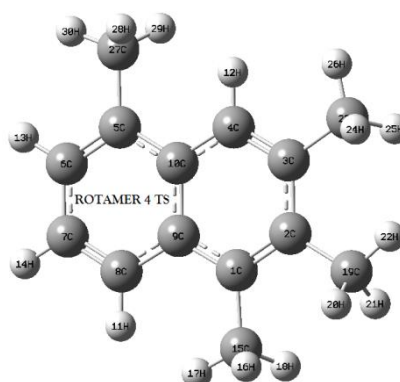
(e) Transition structure of Rotamer 4

Figure 1. The optimized geometries of the 1,2,3,5-TMN isomer and transition state structures of rotamers at the B3LYP/cc-pVTZ level, atom numbering and methyl group rotation angles.
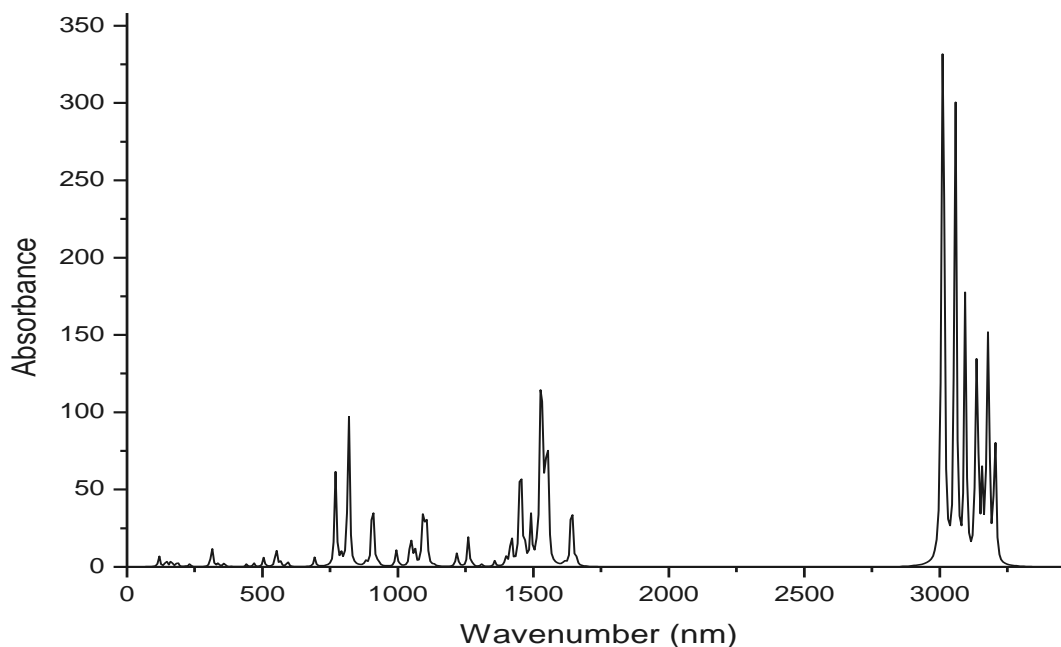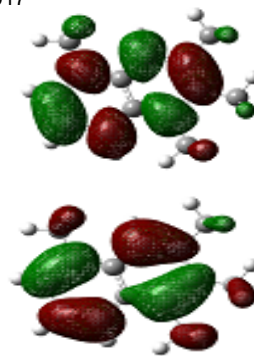
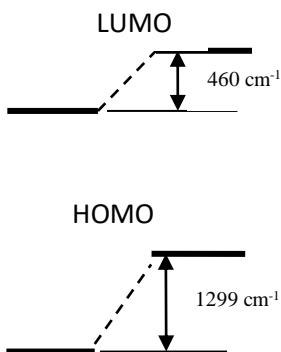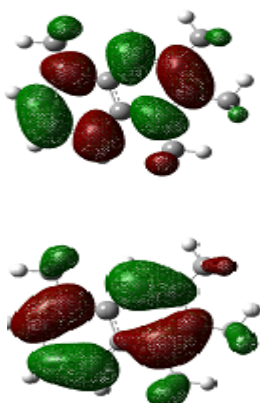**Figure 2 : The theoretical IR spectrum of 1,2,3,5-tetramethylnapthalene**
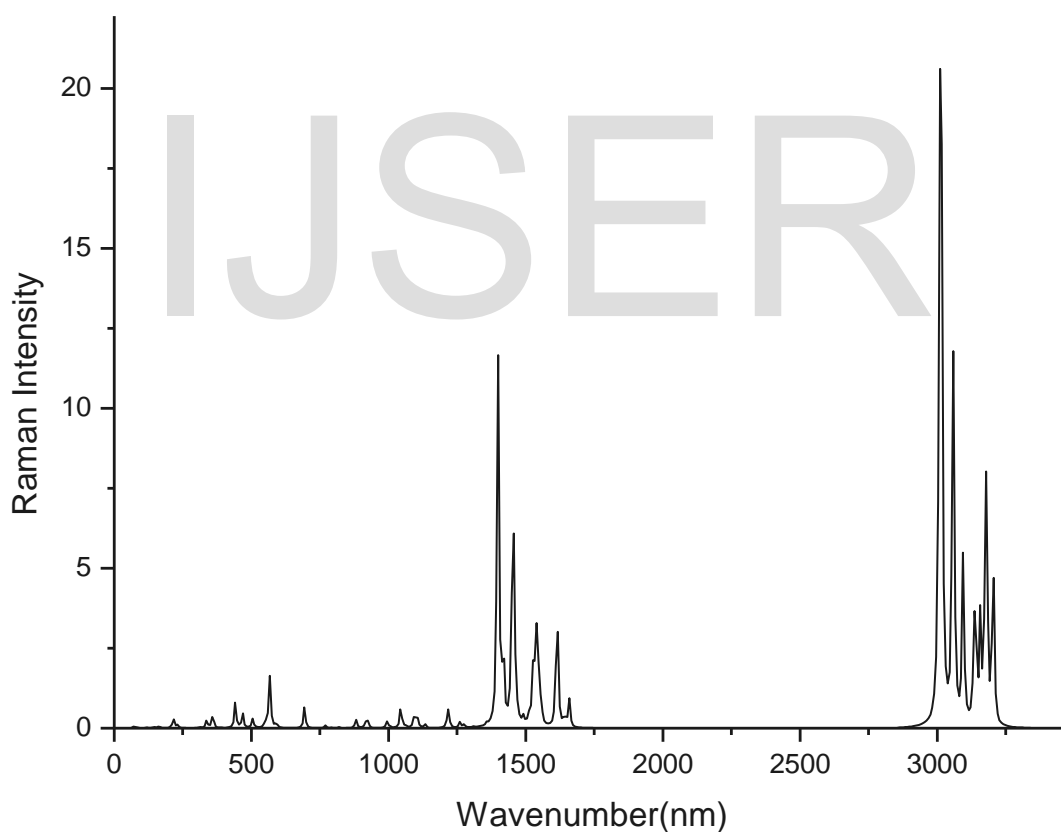
Figure 3 : The theoretical Raman spectrum of 1,2,3,5- tetramethylnapthalene
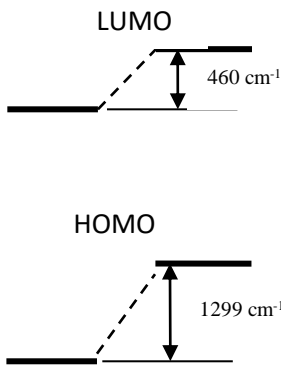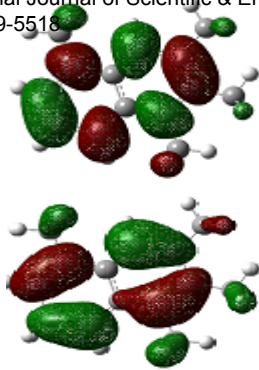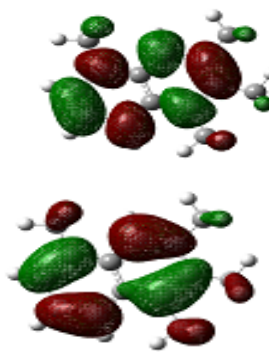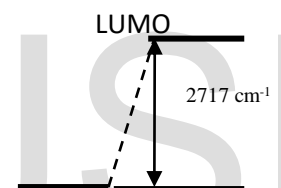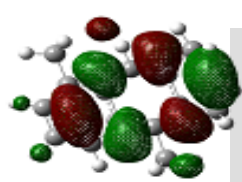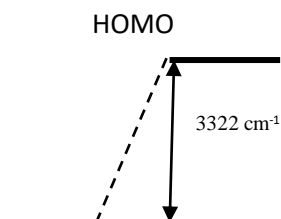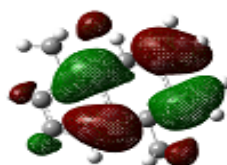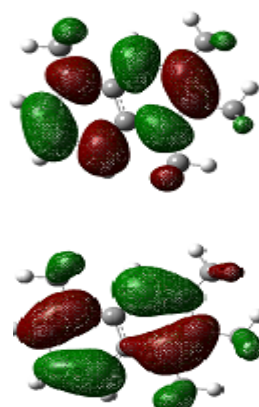
Figure 4. Electron density plots of HOMOs and LUMOs of 1,2,3,5-TMN for the minimum energy structures (left) and transition state structures (right).The relative stability of the HOMOs and LUMOs is depicted schematically.